



HAL
open science

Heterogenised Molecular Catalysts for Sustainable Electrochemical CO₂ Reduction

Domenico Grammatico, Andrew Bagnall, Ludovico Riccardi, Marc Fontecave,
Bao-lian Su, Laurent Billon

► **To cite this version:**

Domenico Grammatico, Andrew Bagnall, Ludovico Riccardi, Marc Fontecave, Bao-lian Su, et al..
Heterogenised Molecular Catalysts for Sustainable Electrochemical CO₂ Reduction. *Angewandte
Chemie International Edition*, 2022, 61 (38), 10.1002/anie.202206399 . hal-03781257

HAL Id: hal-03781257

<https://univ-pau.hal.science/hal-03781257>

Submitted on 13 Dec 2022

HAL is a multi-disciplinary open access archive for the deposit and dissemination of scientific research documents, whether they are published or not. The documents may come from teaching and research institutions in France or abroad, or from public or private research centers.

L'archive ouverte pluridisciplinaire **HAL**, est destinée au dépôt et à la diffusion de documents scientifiques de niveau recherche, publiés ou non, émanant des établissements d'enseignement et de recherche français ou étrangers, des laboratoires publics ou privés.

Heterogenised molecular catalysts for sustainable electrochemical CO₂ reduction

Domenico Grammatico,^[1, 2] Andrew Bagnall,^[2, 3, 4] Ludovico Riccardi,^[2, 3, 5] Marc Fontecave,^[6] Bao-Lian Su,^[1] and Laurent Billon^[2]

1. Laboratory of Inorganic Materials Chemistry (CMI), University of Namur, 61 rue de Bruxelles, B- 5000 Namur, Belgium.
2. Bio-inspired Materials Group: Functionality & Self-assembly, Université de Pau et des Pays de l'Adour, E2S UPPA, CNRS, IPREM UMR 5254, 64000, PAU, France
3. Department of Chemistry, Ångström Laboratories, Uppsala University, Box 523, 751 20 Uppsala, Sweden
4. Univ. Grenoble Alpes, CNRS, CEA, IRIG, Laboratoire de Chimie et Biologie des Métaux, 17 Rue des Martyrs, F-38054 Grenoble, Cedex, France.
5. Molecular Materials and Nanosystems, Institute for Complex Molecular Systems, Eindhoven University of Technology, 5600 MB Eindhoven, The Netherlands
6. Laboratoire de Chimie des Processus Biologiques, UMR CNRS 8229, Collège de France-CNRS-Sorbonne Université, PSL Research University, 11 Place Marcelin Berthelot, 75005 Paris, France.

Abstract

In recent years, there has been a rapid rise in interest regarding the advantages of support materials to protect and immobilise catalysts for the carbon dioxide reduction reaction (CO₂RR) within rationally designed local environments in order to overcome the weaknesses of many well-known catalysts in terms of their stability and selectivity.

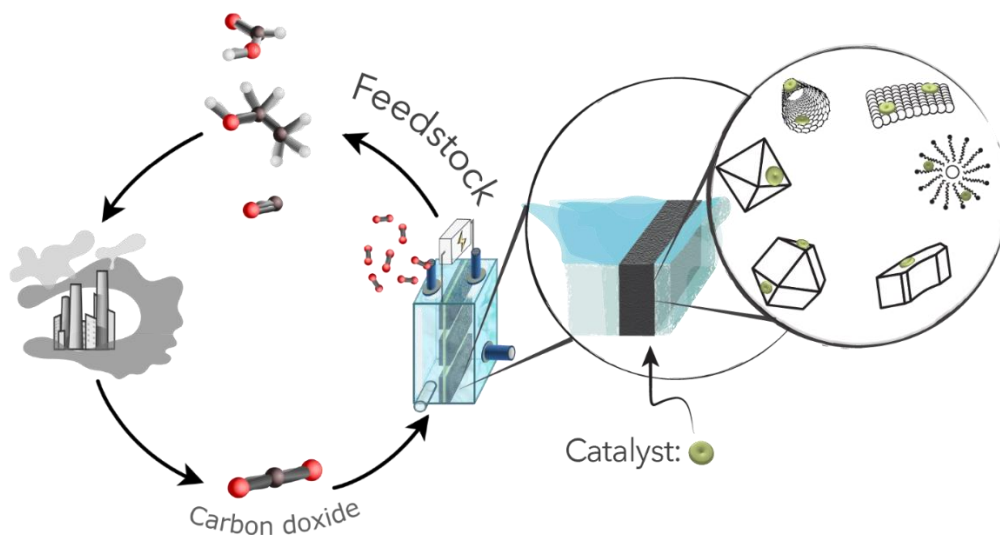
Due to the substantial complexity associated with both controlling the selectivity of the CO₂RR and maximising the stability of the active site through chemical modification of the catalyst alone, such support-focused approaches represent a very promising strategy towards optimising the employment of such catalysts, which, in general, either lack stability and/or selectivity or are based on rare noble metals. In all cases, therefore, maximising the efficiency and robustness of the use of the catalyst is absolutely imperative when considering scalability and viability of devices for CO₂ capture and utilisation (CCU) and CO₂ valorisation. However, the specific effects of the different supports on catalysts' performances in terms of faradaic efficiency, product selectivity, overpotential requirement and obtained current density (versus those of the catalysts used without supports) have often not been directly compared in the literature.

Hence, in this review, direct consideration and comparison of these factors between different catalyst-support systems for the CO₂RR shall be made, with the intention of leading towards standard benchmarking for comparison of such systems across all support strategies, taking into account these multiple pertinent metrics, and also enabling clearer consideration of the necessary steps for further progress.

Finally, a graphical comparison of the reported systems employing molecular catalysts is shown and discussed in order to summarise the current state of the art and give a future perspective of which are the most promising support systems on the basis of the current situation, alongside a final note on the need for development of more advanced experimental and computational techniques in this field to aid the rational design principles that would be prerequisite to prospective industrial upscaling.

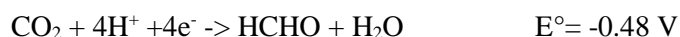
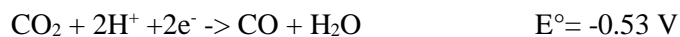
Introduction

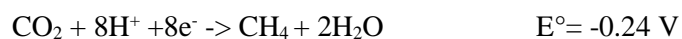
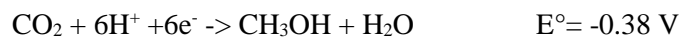
Global warming has been a major growing issue in recent decades and will remain so in the coming years. It has therefore received much attention from the scientific community. CO₂ emissions into the atmosphere have reached excessive levels within the current context. A few years ago, reports announced a concentration of 400 ppm of CO₂ in the atmosphere¹, mainly due to industrial and anthropogenic processes and the use of fossil sources to produce electricity and fuels. A solution is needed to reduce the amount of CO₂ released in order to avert the environmental, ecological and societal consequences of heightened CO₂ levels. There are different ways to reutilise CO₂: microalgae, hydrogen production to convert captured CO₂² and the electroreduction of CO₂ (CO₂RR), which is one of the most promising pathways to reduce the amount of CO₂ while also producing chemicals and products with added value (Scheme 1).



Scheme 1. Schematic summary of the topic of this review article.

Indeed, the CO₂RR is a crucial method to fix the carbon present in the CO₂ into fuels and feedstocks to achieve a negative overall carbon emission. The reduction pathways of CO₂ which produce C₁, C₂ and C₃ products have complex mechanisms due to the stability of the CO₂ molecule. Energy is needed to carry out the reaction, and the use of a catalyst is required because of the inertness of the substrate resulting in high energy barriers.³ Indeed, the one-electron reduction is not favourable and requires a sizeable kinetic overvoltage. The overpotential can be limited with proton assisted reactions, shown in Equation 1. All the potentials are given *versus* the NHE (Normal Hydrogen Electrode) electrode.

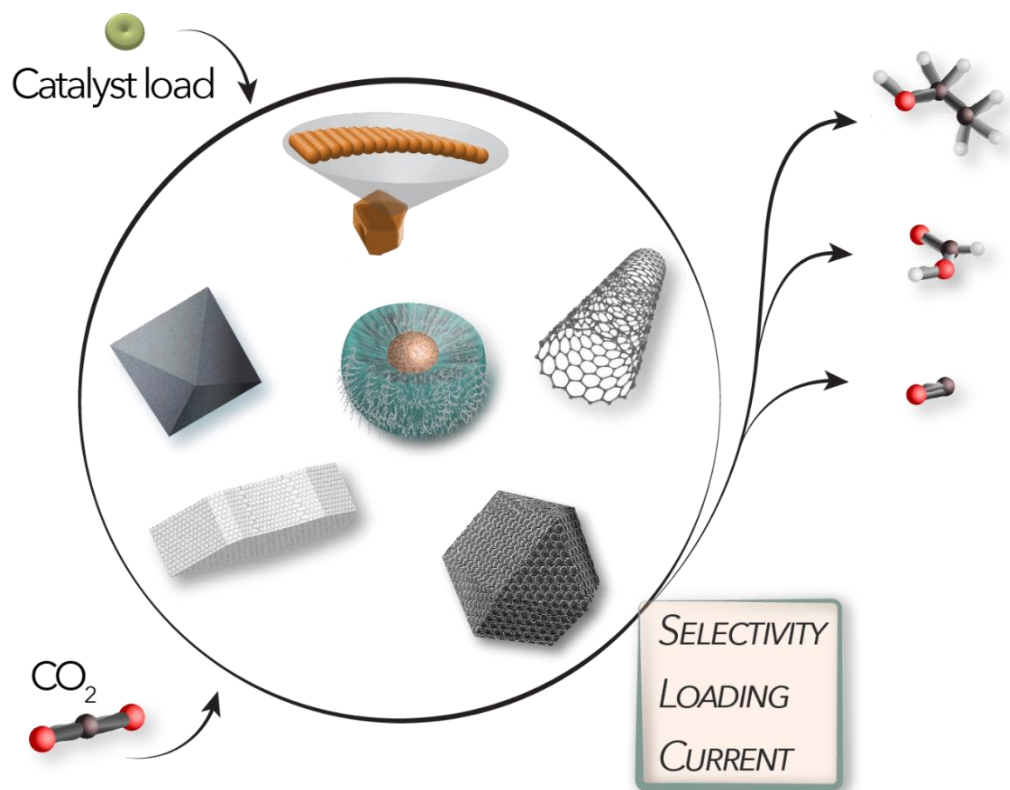




Equation 1: Standard electrochemical potentials for CO₂ reduction³

The obtained products of the electroreduction mainly depend on the catalysts employed. Homogeneous catalysts take part on the reaction in the same phase as the reactants, while in heterogenous catalysis the phases are different. There also exist so-called hybrid systems, in which a molecular catalyst is fixed on a conductive support. In this case the catalyst is heterogeneous in nature and the products obtained and the efficiency of the process strongly depend on the choice of support.

This manuscript reviews the works present in the literature for the CO₂RR using molecular complexes as active sites heterogenised on a variety of supports, highlighting the influence and importance of the support and the local medium. Indeed, heterogeneous catalysts are preferable because of the simplicity in the design of the reactor and the ease in further separation and handling of the products, as well as stability and reusability.⁴ Industrially, the chance to reuse the catalyst drastically affects the costs to improve the economic competitiveness of the process⁴. Combining the unique properties of homogeneous catalysts with specific heterogeneous features can lead to an optimised process (Schemes 1 and 2). Heterogenisation *via* immobilisation of molecular complexes in and on the electrode for the CO₂RR could lead to an efficient and scalable system, reducing the applied overpotential needed, increasing the current density and boosting the selectivity for a specific CO₂RR product(s). Currently, this strategy presents a significant challenge, but also opportunities to explore new concepts, technologies, industries, and research. Supported and immobilised catalysts represent an excellent trade-off strategy. The most recent advances (Table 1) will be described and analysed, focusing on the different supports and their role in the CO₂RR efficiency.^{5,6}



Scheme 2. Schematic summary of some of the supports considered in this review article.

Table 1. Performances of the reported hybrid systems for CO₂RR described in this work

| Support | Active sites | Loading | Potential (V vs RHE) | Current density (mA*cm ⁻²) | FE for main products | Time (h) | Ref. |
|-------------------------|---------------------------------------------------------------------|----------------------------|----------------------------------------|----------------------------------------|------------------------------------|----------|------|
| Carbon | | | | | | | |
| CNTs-OH* | Co porphyrin | 60 μg*cm ⁻² | -0.65 | 6 | CO=90% | 12 | [51] |
| Py-CNTs* | CoPc | 5 nmol*cm ⁻² | -0.73 | 10 | CO=90% | 12 | [46] |
| MWCNTs* | [Co(qpy)] ²⁺ | 8.5 nmol*cm ⁻² | -0.53 | 11.9 | CO=100% | 4.5 | [18] |
| CNTs* | Fe porphyrin | 2.4 mol*cm ⁻² | -1.03 | 0.5 | CO=96% | 7 | [52] |
| CNTs* | Co(TPP) | 3.4 nmol*cm ⁻² | -0.24 | 3.2 | CO=80% | 4 | [16] |
| MWCNTs * | Ni cyclam | 5 nmol*cm ⁻² | -2.54 Fc ⁺ /Fc ⁰ | 10 | CO=90% | 4 | [44] |
| MWCNTs* | Co(TPP) | 0.67 nmol*cm ⁻² | -1.35 | 3.7 | CO=98% | 4 | [47] |
| SWCNTs* | Co(TPP) | 0.11 nmol*cm ⁻² | -1.35 | 3.7 | CO=85% | 4 | [47] |
| RGO* | CoPc | - | -0.59 | 1.5 | CO=74% | 10 | [26] |
| CB* | CoPc | - | -0.59 | 1.7 | CO=65% | 10 | [26] |
| CNTs* | CoPc | 18 nmol*cm ⁻² | -0.59 | 6 | CO=94% | 10 | [26] |
| CNTs* | CuPolyPc | - | -0.7 | 7.5 | CO=80% | 50 | [54] |
| CNF* | CuPolyPc | - | -0.7 | 5 | CO=5% | - | [54] |
| PG* | InPP | 13 nmol*cm ⁻² | -1.5 | 17 | HCOOH=100% | 1.5 | [55] |
| GC* | InPP | 13 nmol*cm ⁻² | -1.5 | 2.5 | HCOOH=18% | 1.5 | [55] |
| BDD* | InPP | 13 nmol*cm ⁻² | -1.5 | 10 | HCOOH=48% | 1.5 | [55] |
| rGO* | CoPc | 38 nmol*cm ⁻² | -0.88 | 20 | CO=85% | - | [57] |
| DrGO* | CoPC | 53 nmol*cm ⁻² | -0.8 | 30 | CO=90% | 20 | [57] |
| GMC* | [Cu ₂ (NTB) ₂ Cl ₂] ²⁺ | 220 nmol*cm ⁻² | -1.278 | 10 | C ₂ H ₄ =42% | 2 | [50] |
| MWCNT* | [Cu ₂ (NTB) ₂ Cl ₂] ²⁺ | 220 nmol*cm ⁻² | -1.278 | - | C ₂ H ₄ =18% | - | [50] |
| GO* | [Cu ₂ (NTB) ₂ Cl ₂] ²⁺ | 220 nmol*cm ⁻² | -1.278 | - | C ₂ H ₄ =10% | - | [50] |
| HPC " | [Rebpy(CO ₃)]Cl | 20 nmol*cm ⁻² | -2.05 Fc ⁺ /Fc ⁰ | 11 | HCOOH=80% | | [13] |
| HPC " | [Rebpy(CO ₃)]Cl | 20 nmol*cm ⁻² | -1.75 Fc ⁺ /Fc ⁰ | 2 | CO=80% | 5 | [13] |
| MOF/COF | | | | | | | |
| MOF-525 * | Fc porphyrin | 62 nmol*cm ⁻² | -1.3 | 2.3 | CO=54% | 3.2 | [61] |
| M-TCPP* | Co porphyrin | - | -0.8 | 17 | CO=98.7% | 36 | [64] |
| COF-366 | Co porphyrin | - | -0.67 | 80 mA*mg _{Co} ⁻¹ | CO=90% | - | [69] |
| COF-366* | Co porphyrin | - | -0.76 | 45 mA*mg _{Co} ⁻¹ | CO=90% | 24 | [39] |
| COF-366-F* | Co porphyrin | - | -0.67 | 65 mA*mg ⁻¹ | CO=87% | 12 | [39] |
| Defected-PON* | CoPc | 110 nmol*cm ⁻² | -0.61 | 8 | CO=97% | 20 | [63] |
| Titania | | | | | | | |
| TiO ₂ * | CoTPP | 17 nmol*cm ⁻² | -1.3 | 1.2 | CO=24% | 4 | [74] |
| TNT* | CoTPP | 40 nmol*cm ⁻² | -1.1 | - | CO=40% | 4 | [75] |
| Meso-TiO ₂ * | MnP | 34 nmol*cm ⁻² | -1.7 Fc ⁺ /Fc ⁰ | 0.6 | CO=70% | 2 | [77] |
| Meso-TiO ₂ * | CoPc | 24 nmol*cm ⁻² | -1.08 | 1.3 | CO=85% | 10 | [78] |
| Polymer-gel | | | | | | | |
| PS-PEO-PS BMIM " | [Rebpy(CO ₃)]Cl | - | -2.1 Fc ⁺ /Fc ⁰ | 0.08 | CO=90% | 1 | [40] |
| Acrylamide BMIM * | [Rebpy(CO ₃)]Cl | 2.24 nmol*cm ⁻² | -0.68 | 1.08 | CO=92.1 % | 24 | [25] |

| | | |
|-----------------------------------------------------------------------------------|----------------------------------------|-------------------------------------------|
| <i>CNTs: carbon nanotubes</i> | <i>GO: graphene oxide</i> | <i>CNF: carbon nanofiber</i> |
| <i>MWCNTs: multi-wall carbon nanotubes</i> | <i>HPC: hierarchical porous carbon</i> | <i>PG: basal-plane pyrolytic graphite</i> |
| <i>SWCNTs: single-wall carbon nanotubes</i> | <i>PON: polymer organic network</i> | <i>GC: glassy carbon</i> |
| <i>RGO: reduced graphene oxide</i> | <i>TNT: Titania nanotubes</i> | <i>BDD: boron-doped diamond</i> |
| <i>CB: carbon black</i> | <i>BMIM: butyl-methyl imidazolium</i> | <i>DrGO: defect rich graphene oxide</i> |
| | | <i>GMC: graphitic mesoporous carbon</i> |
| | | |
| <i>Pc: phthalocyanine</i> | | <i>* : aqueous media</i> |
| <i>TPP: tetraphenyl porphyrin</i> | | <i>' : organic solvents</i> |
| <i>PP: protoporphyrin</i> | | <i>“ : ionic liquids</i> |
| <i>MnP: fac-[MnBr(4,4'-bis(phosphonic acid)-2,2'-bipyridine)(CO)₃]</i> | | |
| <i>bpy: 2,2'-bipyridine</i> | | |

Active sites for CO₂RR

The metal centre and structure influence the catalytic system employed, resulting in specific selectivity for certain products and reaction efficiency. Transition metal complexes with earth-abundant and rare metals have been extensively studied in the past.^{7,8} The catalysts used can be divided mainly into three groups: metal catalysts with macrocyclic ligands, metal catalysts with bipyridine ligands, and metal catalysts with phosphine ligands, all of which bind different metals. From the beginning of these studies, nickel (Ni) and cobalt (Co) were the first metals employed in metal complexes with different macrocyclic ligands. These complexes can catalyse the reduction of carbon dioxide to carbon monoxide or a combination of molecular CO and H₂ at potentials ranging from -1.3 to -1.6 V *vs* SCE. High current efficiencies of up to 98% were reached, corresponding to only low turnover frequencies of between 2 and 9 per hour at room temperature⁹. Again, using nickel as the metal and focussing on cyclam complexes, Kubiak and co-workers have studied a highly efficient system for the production of CO from an unsubstituted Ni(cyclam) complex, showing the possibility for attenuation of the activity through methyl substituents on the amine groups of the cyclam ring. Iron-based molecular complexes are often used to catalyse CO₂RR, especially iron (0) porphyrins (tetraphenyl porphyrin - TPP) can work as a suitable catalyst for the reduction of CO₂ to CO.¹⁰ In addition to these non-noble metals, a more expensive metal such as rhenium, typically with a bipyridine ligand, can also be used to produce CO and, in some instances and particular conditions, formate with high efficiency and selectivity.¹¹⁻¹³ Conversely, formate is obtained with high selectivity and efficiency by employing molecular catalysts containing rhodium (Rh) or iridium (Ir).

Immobilisation strategy and supports

In order to advance the application of molecular catalysts, there is a need to realise systems that can be upscaled and implemented in industrial devices.¹⁴ Following these needs, scientific research is moving toward the development of solid hybrid systems. Herein, only the immobilisation of active molecular species on support materials and their influence on the CO₂RR shall be described.

Several support materials are used in the literature, such as carbon-based supports, titania-based supports, and polymer-ion gels. Moreover, multiple strategies of immobilisation can be exploited to tune the

properties of the heterogeneous system. The method of immobilisation also influences the performance and efficiency of the system. Different strategies are described in the literature, such as grafting *via* covalent bonding, immobilisation *via* weak interactions and physical adsorption, and integration of the molecular complexes into the porous support structure. Each strategy has its own advantages and drawbacks.

The easiest immobilisation method employs physical adsorption through non-covalent interactions such as π - π stacking and electrostatic interactions. The main advantage here is the ease and the rapidness of the technique. Indeed, no significant additional synthetic steps are needed.^{15,16,17,18} High amounts of molecular complexes can be loaded to achieve a high turnover frequency (TOF), the value conventionally used to measure the instantaneous efficiency of a catalyst as the number of turnover per unit of time and active sites.¹⁹ However, such non-covalent interactions are well known to be comparatively weak, and the active sites may accordingly easily leach out and detached from the support after being exposed to solvents and/or a harsh environment.¹⁷

A more rigorous strategy for immobilisation is to form a covalent bond or bonds between the molecular complex and the support. This scenario often consists of an initial functionalisation of either the support or the ligand, leading to a lengthier and more complex process. Several functional moieties can be utilised to graft complexes, such as diazonium²⁰, phosphonic acid²¹ and thiol groups.²² These kinds of grafting are more durable and robust than the non-covalent ones, but on the other hand, more than one layer of catalyst is often attached unintentionally, leading to insulation and mass transfer issues.²³

Another strategy described here employs direct immobilisation of molecular complexes inside Covalent Organic Frameworks (COFs) or Metal-Organic Frameworks (MOFs).²⁴ These organic frameworks can be exploited as support in two ways: by covalent immobilisation through the linkers of the frameworks or not covalent by immobilising the active species within their pores. This strategy has the advantage of avoiding the use of separate support structures since the frameworks themselves can be conductive and act as a support. The porosity of the 3D structures also allows high loadings of active sites, a key benefit of this approach.²⁵ The same considerations as for the chemical bonding immobilisation strategies also apply: in this case, the synthesis and insertion of the modified linker within the framework might be a complicated procedure.

There also exist strategies whereby catalysts can avoid any interaction with the support: for example, catalysts can be trapped on a polymer matrix in gel form.²⁶

In all these strategies, the support employed plays a fundamental role, since is always present in heterogeneous system²⁷, in the global activity of the catalyst. There are different properties which have significant impacts: porosity (which can improve the mass transfer), the degree of the hierarchy of the porosity, and the conductivity (which improves the transfer of electrons). Several supports have already been studied and described in the literature to tune these properties and improve the system's efficiency.

Carbon materials in all their possible forms are the most used support, mainly on account of their conductivities. Among these, carbon nanotubes^{27,28,18,29,30} are the most commonly used, followed by carbon cloth^{31,16,32}, graphene^{33,34,35} and carbon derived from sacrificial MOF skeleton.^{13,36}

Among the inorganic materials widely used are titania^{37,21,38} supports, which exploit their porosity to improve mass transfer.

The most relevant supports described in this article are summarised in Figure 1.

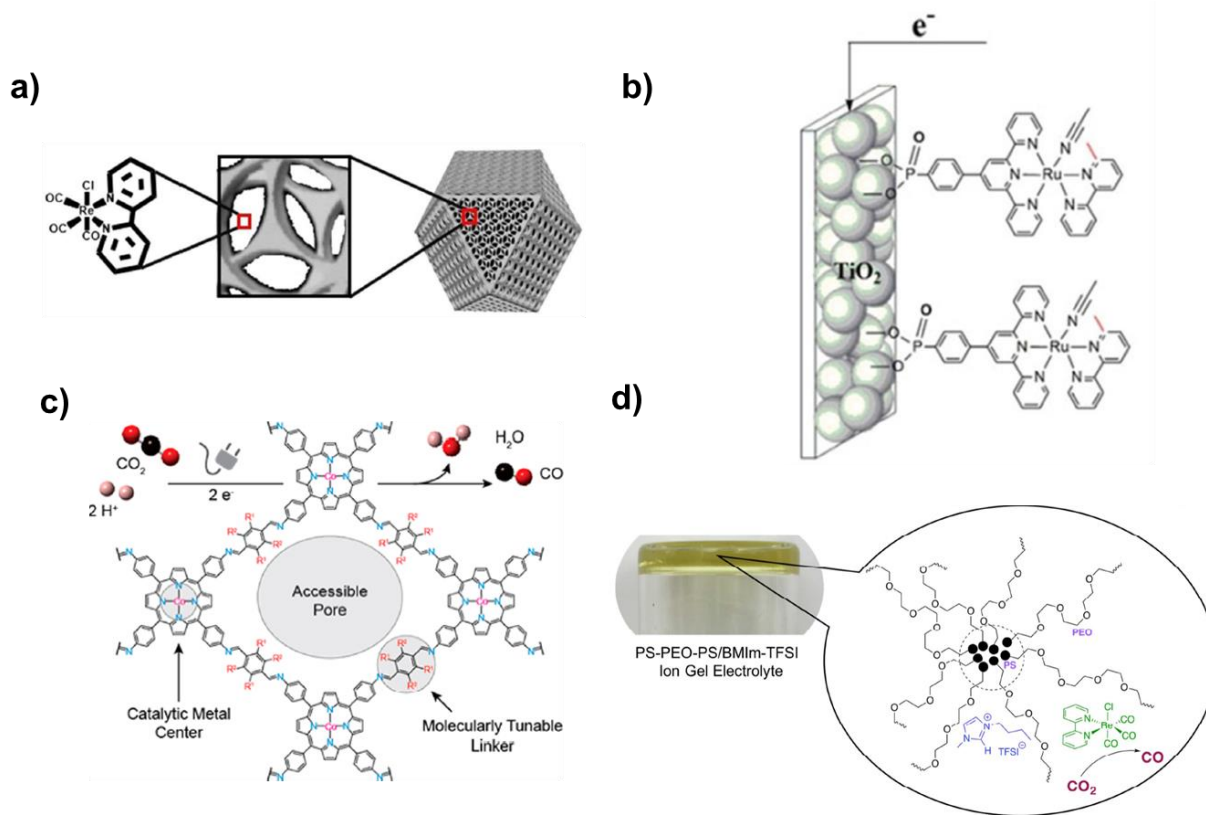


Figure 1. Summary of the most relevant work presented in this review for each support considered: a) from Immobilisation of a molecular Re complex on MOF-derived hierarchical porous carbon for CO₂ electroreduction in water/ionic liquid electrolyte¹³ B) from Electro-catalytic CO₂ reduction with a Ruthenium catalyst in solution and on nanocrystalline TiO₂³⁹ C) from Reticular electronic tuning of porphyrin active sites in covalent organic frameworks for electro-catalytic carbon dioxide reduction⁴⁰ D) from Electro-catalysis of CO₂ reduction in brush polymer ion gels.⁴¹

Carbon-based supports. Among all the supports described in the literature, carbon-based materials are the most widely used. Their high electrical conductivity makes them one of the first choices as a support for heterogeneous catalysts for the CO₂RR. Different features and parameters of the carbon support need to be considered to enhance the catalytic activity. Firstly, the aforementioned electrical conductivity is needed to improve the total charge passing through the system. Secondly, the high surface area and the porosity serve to avoid mass transfer problems caused by the low solubility of CO₂ in aqueous electrolytes and tend to enable immobilisation of a higher number of active sites. Finally, hydrophobicity³⁶ has a crucial role in trapping the gas and increasing the concentration of CO₂ in the vicinity of the electrode.⁴² The chemical structure and the morphology of the carbon support significantly impact the catalytic performance (Figure 2).⁴³ Recently, the use of carbon nanotubes (CNTs) has achieved widespread popularity. CNTs are widely used in both the forms of single and multi-wall nanotubes, SWCNT and MWCNT, for their high conductivity and stability. Although their main drawback is their inherent catalytic activity for the undesirable proton reduction reaction^{29,44}, they are widely employed because of their aforementioned properties. Several catalysts have been tested for CO₂ electroreduction and heterogenised using CNTs, in all the cases improving the results. The influence of CNTs acting as the support for the catalyst in enhancing the activity and selectivity for CO₂RR has been attributed to (i) the presence of surface functional group, as -OH, -NH and -pyridine which can affect the surrounding electron densities;⁴⁵⁻⁴⁶ (ii) the influence of the curvature of the CNTs in favouring different products at different overpotentials by altering the interactions between catalysts and CNTs²⁷⁻⁴⁷; (iii) the microporosity of the CNTs influencing the mass transport and the concentration of CO₂ present at the surface and in contact with the catalyst, thereby impacting the catalytic activity⁴⁸.

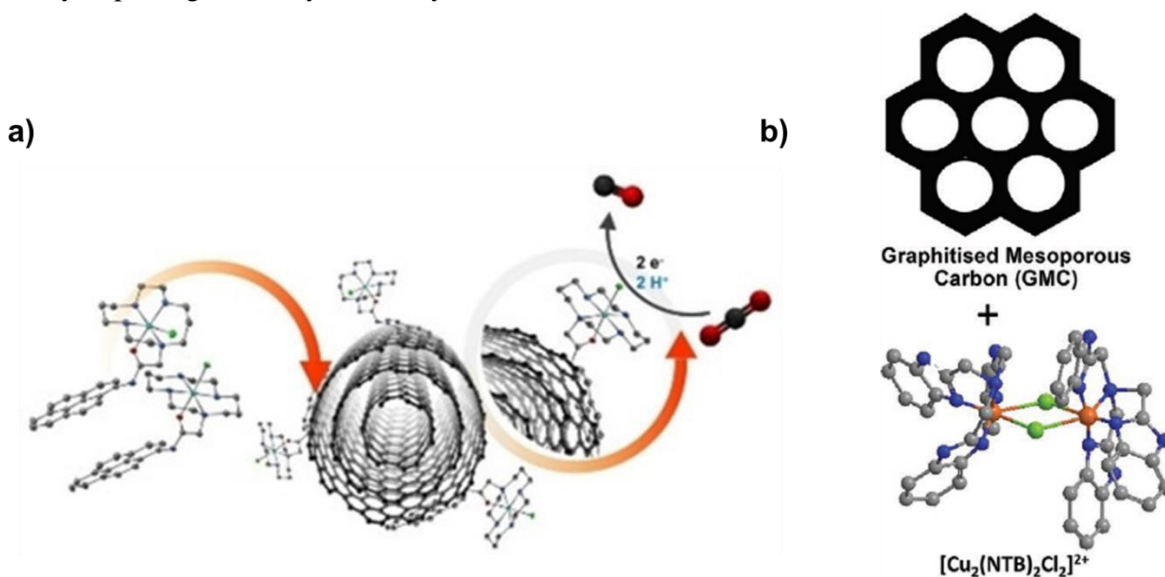


Figure 2. a) Nickel cyclam Supported on MWCNTs⁴⁴ and b) a bimetallic Cu complex employed as CO₂ reduction catalysts by immobilisation on graphitised mesoporous carbon.⁴⁹

Starting with the importance of the chemical modification of the support, Zhu *et al.*⁵⁰, covalently grafted a cobalt porphyrin (CoPP) on CNTs. The CNTs were previously functionalised to contain hydroxyl groups which made up 3.06% of their total weight. A theoretical monolayer of CoPP was added to the CNTs, detected *via* Inductively coupled plasma (ICP) and resulting in a loading of 10 wt% of CoPP. The successful linkage of the molecular complexes with the CNTs was proved by spectroscopic analysis. The hybrid

electrode, denoted CoPP@CNT, was tested for the CO₂RR. The sample was stable at all potentials investigated, reaching up to 90% FE for CO and around 6 mA.cm⁻² at -0.65 V vs RHE in aqueous media. When compared with the CoPP molecular complexes immobilised on CNTs without -OH groups, this result shows a significant improvement in terms of current density: thus proving the importance of the hydroxyl functionalisation in enabling the covalent grafting. The -OH functionalisation dramatically enhances the loading of the molecular complex immobilised and avoids agglomeration on the surface, which is likely to limit the mass transport and negatively influence overall efficiency.⁵⁰ The same research group⁴⁶ also investigated a different functionalisation on the CNT support. A pyridine moiety was appended to the surface of the CNT (py-CNT), exploiting the reduction reaction of diazonium species. The N atoms on the pyridine were detected by Raman spectroscopy and XPS measurements (Figure 3 a and b). This time, the support was then loaded with a certain amount of cobalt phthalocyanine (CoPc) by axial coordination through a bond between the Co centre in CoPc and the nitrogen atom in the py-CNT. Comparing the bare CoPc, the CoPC@CNTs and the CoPc@py-CNTs, the latter showed the highest current density: 10 mA cm⁻² at -0.73 V vs RHE, corresponding to a FE for CO of more than 90%.

Ming Hu *et al.* chose to immobilise cobalt porphyrin (CoTPP) on carbon nanotubes. This work demonstrated the potential of the heterogenisation process to enable working in aqueous media, as well as the importance of the support structure in influencing the reaction mechanism and the activity of the catalyst itself. The current reached was 3.2 mA cm⁻² with a good CO FE of around 80% throughout a 4 h bulk electrolysis experiment, at an applied potential of -1.35 V vs SCE. The CoTPP, after immobilisation, can activate the CO₂ and produce CO at low applied overpotentials. Under homogenous conditions in DMF, two electrons are needed to activate and reduce CO₂ with [Co(0)TPP]²⁻, but this demands high applied overpotentials that lead to deactivation. In this case, the immobilisation plays a fundamental role in the formation of the active species with high activity for CO production.¹⁶

As previously mentioned, the curvature of the CNTs is a crucial feature. A recent study by Chen *et al.* combines experimental and computational methods to illustrate the influence of the support when Co(TPP) is stacked on CNTs.⁴⁷ However, the turnover frequency (TOF), decreases, even if more catalyst is loaded. The system is likely to agglomerate and reduce the amount of available active catalyst. Using molecular dynamics (MD), the Co(TPP)/CNTs system was studied. MWCNTs and SWCNTs were used, with diameters of 60/130 Å and 12/15 Å, respectively, with distinct surface areas. Although logically, MWCNTs are supposed to be inferior support, since their surface area is lower than that of SWCNTs, similar current densities are obtained from both supports, and in fact, higher FEs and higher TOFs are obtained for the Co(TPP)/MWCNTs system when the same amount of catalyst is loaded. Thus, the authors claim that the aggregation of catalysts on the surface is probably more favourable on the SWCNTs. This difference in reactivity between the systems based on the two different supports has been attributed to the lower curvatures of the MWCNT samples. This is because Co(TPP) can dimerise due to its porphyrin ring, which facilitates intra-species π - π interactions as well as π - π interactions to the support. This kind of dimerisation may therefore be provoking competition between the Co(TPP)/CNTs interactions and the Co(TPP)-Co(TPP) intermolecular interactions.⁴⁷

Interestingly, the current density increases further when a more cathodic potential is applied for the CoPc@py@CNTs than for the CoPc@CNTs. A mechanism for the reaction was also proposed based on the calculated Tafel plots (Figure 3 c). The Tafel slope of the CoPc@py@CNTs is around 60 mV.dec⁻¹ less than the non-functionalised system, with transport limitation issues occurring. Both systems have the same rate-determining step (RDS), which is shown to be the binding of CO₂ in Figure 3 d. Nevertheless, coordination between Co and N is likely to be stronger than the Van der Waals (VdW) interactions between CoPC molecules themselves. Concerning these molecules, the coordination to the metal centre increases

the charge density of the system, increasing the nucleophilicity of the metal centre, allowing it to more strongly bind the CO₂, which is the rate-determining step (RDS), and this, therefore, promotes the CO₂RR.⁴⁶

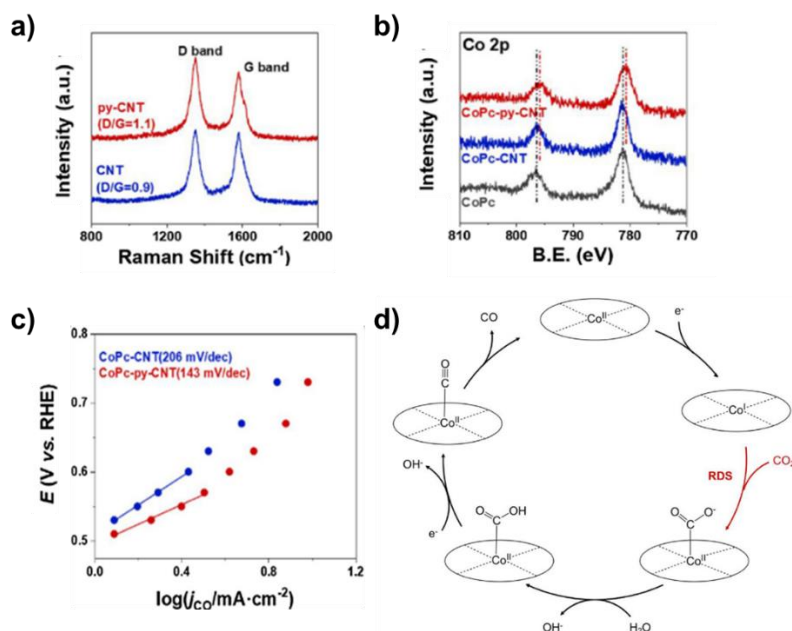


Figure 3. a) Raman spectrum of py-CNT and pristine CNT and (b) Co 2p spectra of free-standing CoPc, CoPc-CNT and CoPc-py-CNT. C) Tafel plots for CoPc-CNT and CoPc-py-CNT at CoPc loading of 5 nmol·cm⁻² and d) proposed Mechanism for CO₂ electroreduction to CO over a catalyst of immobilised CoPc on CNT.⁴⁶

It has been further shown by Zhang *et al.* that the form of the carbon support drastically influences the catalytic activity and the selectivity.²⁸ They used CoPc as a catalyst loaded on reduced graphene oxide (RGO), carbon black (CB) and finally on CNTs. Lower current densities were found for the RGO and CB systems when loading the same amount of catalyst. Moreover, the FE toward CO with the CNTs was 10% higher than the others. Finally, stability experiments of the system were also performed, showing that the RGO and CB systems have lower catalytic stability than CNTs.²⁸ Thus, it was clear that an enhanced catalytic performance could be achieved by using CNTs. In this study, the CNTs were of a higher graphitic degree than the other two supports employed. The higher graphitic degree is likely to favour the π - π interactions with the catalyst and facilitate the electron transfer.⁵¹ A similar approach was followed by Karapinar *et al.*⁵² where a polymer of Cu phthalocyanine (CuPolyPC) was coated on CNTs and carbon nanofiber (CNF). While CuPolyPC@CNT reached around 85% FE for CO and a current density of 7.5 mA·cm⁻² at -0.7 V vs RHE, the CuPolyPC@CNF generated mostly H₂ with a lower current density. This difference was attributed to the higher surface area, the higher electrical conductivity of CNTs, and a better interface of the Cu active sites which were attached to the CNTs.

Wang *et al.* used a cobalt catalyst to prepare a supported catalyst bearing a cobalt quaterpyridine (qpy) at the surface of MWCNTs. An ink was readily prepared by adding the [Co(qpy)]²⁺ to the MWCNTs suspension. The ink was then drop-cast onto different carbon supports. The concentration of the active

complex on the electrode was quantified electrochemically, showing a lower quantity of the active species than the one loaded directly. The lower active concentration is likely provoked by the high amount of catalyst loaded into the porous framework, thus leading to saturation and agglomeration. The electrode produces CO with a FE close to 100% at an applied potential of -0.53 V vs RHE in 0.5 M NaHCO₃, reaching the best current density of 11.9 mA cm⁻² for 8.5 nmol cm⁻² of loading. The supported system competes well with the best molecular catalysts assayed in water for the CO₂RR.¹⁸ It, therefore, successfully exploits the advantages of the adsorption of the [Co(qpy)]²⁺ on the surface of the carbon support, such as stability and activity in aqueous media. From the same group, an Iron-based molecular complex was immobilised on the surface of the CNTs, exploiting a pyrene moiety to anchor it onto the carbon support *via* π - π interactions, enabling the use of the complex in aqueous media for the CO₂RR to CO with 96% FE, thanks to the heterogenisation of the catalyst.⁵³ These two works highlight the versatility of the strategy, being efficient with different catalysts.

Nickel cyclam is another well-known molecular catalyst, active for the CO₂RR. However, it often necessitates the employment of a Hg electrode. Pugliese *et al.* developed a new nickel cyclam molecular complex with an appended pyrene moiety to immobilise the active site on CNTs and investigate its efficiency for the CO₂RR without involving any mercury electrodes. The molecular complex was shown to be very selective for CO, with around 96% FE in DMF/H₂O media, but, as already shown previously, only a low current is obtained with a glassy carbon electrode. Once immobilised through non-covalent interactions on the surface of the MWCNTs, the system retains its selectivity and achieves a drastically increased current density, reaching 10 mA cm⁻², compared to the 0.3 mA cm⁻² from a 10 mM solution of the complex. This remarkable result highlights the stable and efficient interaction of the complex with the MWCNTs, which favours the active conformation of the complex. The large surface area and the organisation of the MWCNTs support structure enhance the properties of the electroactive sites. The use of more porous supports with enhanced structuration may, in this case, improve the system yet further.⁴⁴

A study of the influence of different substrates was also carried out by Birdja *et al.*⁵⁴ In this case, an indium (III) protoporphyrin (InPP), selective for formic acid production, was heterogenised in different substrates to investigate their influence. Moreover, the surface of the supports was also modified by electrochemistry and plasma. Basal-plane pyrolytic graphite (PG), glassy carbon (GC) and boron-doped diamond (BDD) were used with and without pretreatments. The heterogenisation process was done by drop-casting the solution of the molecular complex on the surface of the substrate, adsorbing the molecular complex through π - π interactions, and was kept constant in all the systems. After controlled-potential electrolysis, the PG substrate was shown to have the most efficient FE for HCOOH and current density, reaching almost 100% of FE and 17 mA.cm⁻² at -1.5 V vs RHE. The current density was normalised by the indium content. Indeed, the substrates have different abilities to heterogenizing the molecular complex. It was shown that PG could host a higher amount of InPP and have a higher saturation limit than the other substrates.

Interestingly, a higher amount of H₂ was detected using InPP-GC comparing with InPP-PG. In addition to that, a higher amount of CO₂ was consumed by the PG system. This feature is attributed to the more efficient mass transfer thanks to the higher porosity of PG than GC or BDD. The GC substrate shows the lowest performance, likely because of its poor permeability of gases and its poor crystallinity. Also, the low efficiency for CO₂RR of GC is attributed to its higher activity for hydrogen evolution reaction (HER) than PG and BDD. The study proves the influence of the substrate's morphology, porosity, crystallinity, and HER activity on CO₂RR efficiency.

The introduction of dopants into the carbon substrate was also investigated by Wang *et al.*⁵⁵; in this work, graphitic sulfoxide and carboxyl dopants of graphene are likely to improve the molecular complex's binding

affinity through axial coordination, which enhances the CO₂RR of the active site. A cobalt-based naphthalocyanine was used (NapCo), which already has a strong capability for π - π stacking with the carbon matrix. Moreover, the coordination with the dopants boosts the immobilisation of the catalyst as well as the CO₂RR itself. The sulfoxide dopants also promote the electron transfer between the substrate and the active sites when compared to carboxyl dopants. The system shows 97% FE for CO at -0.8 V *vs* RHE for the NaPCo immobilised on the sulfoxide doped graphene in aqueous media. The TOF was increased 3 times compared to the carboxyl dopant. In addition to doping and functionalisation of the carbon matrix, Liang *et al.*⁵⁶ studied the influence of defects on the graphene substrate. Cobalt phthalocyanine was used again as a molecular complex and immobilised in reduced graphene oxide (rGO). Firstly the rGO was mixed with dicyandiamide and then a N-removal strategy allowed the introduction of defects. After the treatments, the graphene structure was not modified as seen in SEM and TEM images, however, significant differences were nonetheless highlighted between the bare rGO and the treated one (DrGO). Raman spectroscopy shows an increased disorder in the DrGO alongside a higher amount of amorphous carbon. EPR spectroscopy further confirms the presence of broken bonds, localised on the defects. The two rGOs were impregnated with a solution of the molecular complex in order to carry out the immobilisation.

Interestingly, UV-Vis spectroscopy shows a more significant redshift of the Q bands for the DrGO, which is caused by a more substantial charge transfer between the matrix and the CoPc, resulting in better π - π interactions. XPS highlights the higher electronic communication between active sites and substrate on the DrGO. Electrochemical characterisation of the DrGO-CoPC shows the highest current density, 30 mA.cm⁻² at -0.8 V *vs* RHE with 90% FE for CO in aqueous media. The DrGO leads to better efficiency and activity than the rGO and is an outstanding system compared to other heterogeneous systems employing Co or other metal active sites. Since a bare DrGO leads to poor selectivity toward CO₂ reduction products, the enhancement in activity of the DrGO-CoPC is attributed to the superior electron communication, which is likely to favour the kinetics of the CO₂ reduction process. Indeed, the CVs show that the Co²⁺/Co⁺ wave, which is one critical step in the CO₂ reduction catalytic cycle using Co centre, is positively shifted when CoPC is immobilised on DrGO, suggesting that the process is accelerated. This, process acceleration leads to an improved electrochemical CO₂RR. Once more, the evident influence of substrate in the overall activity and efficiency of the hybrid system is highlighted herein.

As introduced previously, mass transfer is important for maintaining the CO₂ concentration on the surface of the catalyst, particularly in water, where the solubility of CO₂ is low compared to other media such as organic solvents and ionic liquids.⁵⁷ The microporosity of the support has been proven to be crucial in improving the mass transfer⁵⁸. Guo *et al.* studied a nickel molecular catalyst immobilised within various different substrates to understand the phenomena through experiments and theoretical calculations. Indeed, it has been shown that the CO₂ physical adsorption capacity and current density increase as the micropore volume is raised. The theoretical calculations demonstrate that the CO₂ adsorption step is the RDS, which explains why the highest efficiency is achieved by the microporous support, which can capture CO₂ the most efficiently. This example highlights the impact of the porous structure on the catalytic activity while the electronic and chemical structures are controlled. Balamurugan *et al.*⁵⁰ used a Cu-based molecular complex immobilised in a graphitised mesoporous carbon (GMC) in this context. The driving force of the immobilisation was the π - π interactions between the support and the complex which were demonstrated by a shrinking of the typical UV-Vis adsorption band of the Cu complex solution with and without the GMC. The copper molecular complex is known to enhance C₂ products formation when it is dimerised. To investigate the influence of the support, the dimeric complex was immobilised on MWCNTs, graphene oxide and GMC, and the catalytic activity in each case was studied. In CO₂-saturated media, LSVs show higher current density and a clearer catalytic wave with GMC as the support. The hybrid CuGMC system shows the highest FE for C₂ products, namely 42% for ethylene at -1.278 V *vs* RHE in 0.1 M KCl. The

graphene oxide and MWCNTs systems exhibited lower selectivity for C₂ products and higher methane production, with a decreased total selectivity for CO₂ reduction products, in fact favouring the HER. Thus, the porosity influences and improves the C-C coupling during CO₂RR. Indeed, the author puts forward that the local pH could be higher inside the pores and therefore favour the production of C₂ products, which has already been demonstrated for nanoporous copper⁵⁹ and proven by theoretical calculation. It was found that increasing the rotation speed while performing electrochemical studies (using a rotation-ring disk electrode) leads to a decrease in C₂ and methane production by instead favouring CO and H₂ production. Another example where the selectivity and efficiency for CO₂RR were improved by the support in terms of selectivity is shown by Grammatico *et al.*¹³. In this work, the well-known complex [Re(bpy)(CO)₃(Cl)], commonly abbreviated as Re(bpy), has been immobilised into the pores of a novel conductive porous electrode. Interestingly, due to the hierarchical porosity, the molecular complex has been successfully fixed within the pores of the carbon material as is without any synthetic modification, which often leads to practical issues and modifications of the electronic properties of the complex. The carbon materials were synthesised using a ZIF-8 MOF as a carbon template, which had been crystallised around PS spheres and possessed a hierarchical porosity of scales ranging from micro-/meso- to macropores, thereby conferring a high surface area. The successful loading of the Re-complex was proven by several techniques, giving a large value for the area density of electroactive species of 20 nmol.cm⁻², in line with previous results in a similar system.⁶⁰ The system showed high selectivity toward CO₂ reduction products in a water/ionic liquid electrolyte. In the LSV in the CO₂-saturated system, a catalytic wave was detected with an onset potential of -1.55 V *vs* Fc/Fc⁺ not present under N₂ atmosphere. Interestingly the selectivity could be tuned by changing the applied potential. Indeed, around 80% FE for CO was obtained with an applied potential of -1.75 V *vs* Fc/Fc⁺ while with the more cathodic potential of -2.05 V *vs* Fc/Fc⁺ almost 80% FE for HCOOH was obtained. Current densities span from 2 to 11 mA.cm⁻² across the potentials investigated. The formate production was not anticipated, because Re(bpy) is typically selective for CO in organic solvents; furthermore, when Re(bpy) was solubilised in the water/ionic liquid media and a CPE experiment was run, H₂ was the main product detected. This demonstrates clearly, the impact of solid support on the activity and selectivity of the system. The activity is most likely boosted by the hydrophobic local environment of the pores where CO₂ is taken up and, increasing its local concentration. Moreover, mass transfer is less hindered, due to the high porosity.

MOFs and COFs. This chapter will describe MOFs and COFs, which are used as porous supports to heterogenise molecular complexes. Indeed, in contrast with carbon-based materials, MOFs and COFs both provide highly-ordered porous networks that are likely to enhance permeation of the electrolyte. Although electron transport is the limiting factor in using MOFs and COFs, the ability of thin films of MOFs and COFs to facilitate charge transfer has recently been reported (Figure 4). Thus, having an organic framework with redox-active molecular complexes as linkers confers several advantages: high surface area and tuneable porosity of the support, hierarchical porosity to enhance mass transfer properties, easy elemental and physical characterisation both pre- and post-catalysis, easier avoidance of aggregation and deactivation processes, and high loadings of electroactive species.^{61–63} This cursory overview will not cover all of the literature on this branch of CO₂RR research, but the most influential papers will be discussed (Figure 4).

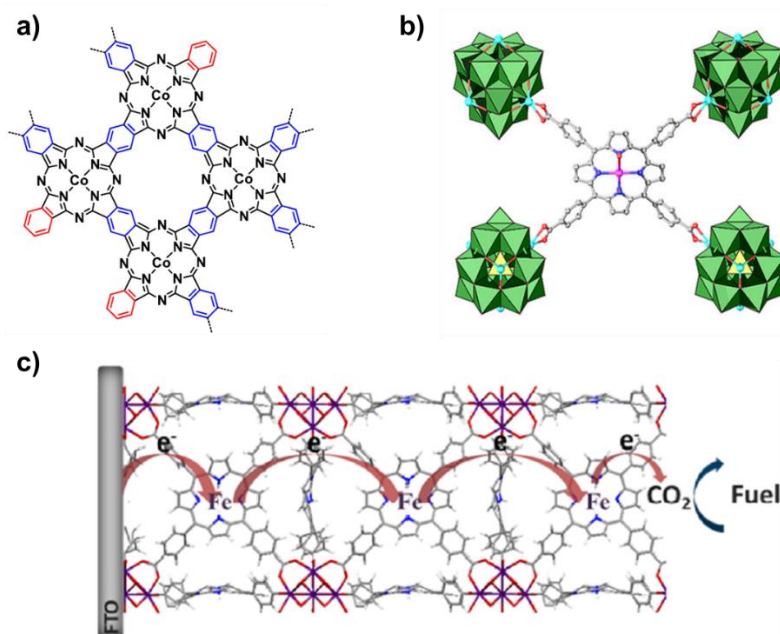


Figure 4. a) defective polymeric Co phthalocyanine (DP-CoPc),⁶⁴ b) Schematic illustration of the structures of M-PMOFs (M =Co)⁶⁵ and c) Fe-porphyrin-based MOF films for electrochemical reduction of CO₂.⁶²

Since the earliest reports of employing MOFs for CO₂RR photocatalysis by Wang *et al.*⁶⁶ in 2011, incorporating noble metals complexes of Ir, Re and Ru into a UiO-67 framework, and then for CO₂RR electrocatalysis by Kumar *et al.*⁶⁷ in 2012, incorporating copper directly within the structure of the Cu₃(BTC)₂ framework, a lot of progress has occurred over the past decade towards incorporating well-established molecular CO₂RR catalysts based on earth-abundant first-row transition metals into MOF supports.

In 2015, Hod *et al.*⁶² incorporated the well-known Fe-porphyrin into a MOF and the system was then studied in the form of a thin-film immobilised on an electrode. The chosen non-metallated porphyrin, MOF-525, has good porosity and outstanding chemical stability for electrochemical studies. The MOF-525 was metallated by post-synthesis modification, reaching an amount of catalyst on the surface three orders of magnitude higher than the previously reported heterogenised molecular complex. Cyclic voltammetry analysis of the Fe_MOF-525 shows an increase in current density in CO₂-saturated solution when compared to under a N₂ atmosphere. The hybrid system reaches a current density of 2.3 mA.cm⁻² in acetonitrile,

achieving 54% FE for CO at -1.3 V *vs* NHE. The overall efficiency was boosted by adding a weak acid, as has previously been reported for homogeneous systems. Indeed, in this case the current density was increased to 5.9 mA.cm⁻² with an associated seven-fold increase in CO production at the same potential after 3.2 hours of bulk electrolysis. The addition of acid also reinforces the electrode's stability. The authors then compared the homogeneous complex with the hybrid system, pointing out a limitation of the Fe_MOF-525 in terms of charge diffusion rather than in terms of the molecular-scale kinetics of the CO₂RR. Indeed, the hybrid electrode shows a 16-times lower TOF than that the homogenous system, but with still two-thirds of the current density, signifying the concentration and immobilisation of the molecular complex on the surface. This work was one of the first attempts to immobilise a molecular complex within a porous MOF structure. Although, the system suffers from limited charge diffusion, it does serve to open the way towards introducing active sites directly as linkers within MOF structures.

In 2018, Wang *et al.*⁶⁵ prepared a series of metalloporphyrins integrated into a MOF structure with a polyoxometallate. Among all the metals studied (cobalt, iron, nickel and zinc), the cobalt-based porphyrin within the MOF shows the lowest required overpotential for catalysis by LSV in a CO₂-saturated atmosphere. Thus, the Co-PMOF system represented the major focus of the study. A FE of 98.7% for CO production was achieved for an applied potential of -0.8 V *vs* RHE in aqueous media, the highest so far among reported MOFs. A current density of around 17 mA.cm⁻² was obtained, with good stability over 36 hours of electrolysis. The fact that Co-PMOF shows the lowest overpotential requirement is taken to indicate favourable kinetics, which may be assigned to more efficient charge transfer and a higher active surface area. The high performances for the CO₂RR are likely to be influenced by the higher efficiencies of the Co-PMOF for both proton and electron transfer compared to the Co-MOF. Indeed, the polyoxometallate is an excellent electron storage system which acts to facilitate the charge transfer. DFT calculations confirm that on bare polyoxometallate (POM) and Co-MOF, the RDS for CO₂RR is the formation of adsorbed intermediates with high free energies. The required (free) energy is decreased when the POM and the Co-MOF are assembled. Thus, these effects are likely due to the efficient synergistic electronic effect of the POM and the central Co-active site. The electronic communication of the POM and the porphyrin within the support MOF structure allows for oriented transport of electrons within the channel, with the result that the MOF is conductive for the transfer of multiple electrons to undergo electrochemical reactions.

Likewise for COFs, intensive research into their application as supports for noble metal-free molecular CO₂RR catalysts has been ongoing in recent years, including from the group of O. M. Yaghi, one of the groups which pioneered reticular chemistry.⁶⁸

Yao *et al.*⁶⁹ pondered combining and testing the CO₂ storage properties of a COF system with the CO₂ electroreduction features of a Co-based molecular complex embedded within the COF structure. A phthalocyanine boronate COF was prepared, and cobalt was employed in the metal active site for the CO₂RR. Firstly, the CO₂ storage properties were tested by evaluating the capability of the material to adsorb certain amounts of CO₂. A trend was identified which indicated the preferable adsorption of CO₂ onto the walls of the pores at lower concentrations. At higher concentrations, the CO₂ was also found in the centre of the catalytic system. It was deduced that the size of the pores in the COF plays a key role: indeed, a smaller pore size COF is more suitable when working at normal (1 atm) CO₂ pressure, whereas at higher pressure, the CO₂ will be distributed uniformly within the pores. Based on this preliminary study, the authors chose a Co-Pc-PBBA (1,4-phenylenebisboronic acid) COF as the electrode for the CO₂ reduction

because of its smaller pore size. Based on the calculations, the onset potential for CO₂ reduction of Co-Pc-PBBA is only 0.30 V, smaller than the bare Co-porphyrin (0.46 V); this is due to the enhanced ability of the COF to adsorb the reaction intermediates. The synergy between the storage and reduction features allows this material to realise competitive performances, achieving a 97.7-times higher local concentration of CO₂ present around the active sites than in conventional aqueous systems. The high local concentration of CO₂ decreases the barriers to the electroreduction reaction, resulting in a lower overpotential requirement and enhanced productivity thanks to the porous, crystalline framework containing the heterogenised molecular complex.

Lin *et al.*⁷⁰ have demonstrated that incorporating a catalytic cobalt-based porphyrin into COFs with copper units is likely to be responsible for enhancing the activity and selectivity for CO of the system. A COF-366-Co was synthesised with Co-porphyrin active sites, which corresponded to 4% of the total cobalt porphyrin present in the whole system. For this system, the current density was found to increase drastically under a CO₂ atmosphere in comparison with the bare carbon electrode, with catalytic onset potential of -0.42 V *vs* RHE in neutral aqueous medium. 90% FE for CO was detected at -0.67 V *vs* RHE for a current density of 80 mA per milligram of cobalt. Moreover, an improvement is observed in the selectivity for CO compared with the molecular system. Long term stability experiments were carried out over 24 hours, showing good stability and significant production of CO over the course of the experiment. This results in substantial improvements in the TOF and TON when normalised to the quantity of molecular cobalt porphyrin. Interestingly, the COF retained its crystalline structure and morphology with no agglomerated Co nanoparticles detected. Hence, the system could be recovered and reused up to 5 times by the authors. The influence of the framework's porosity was further investigated by the substitution of the BDA (1,4-benzenedicarboxaldehyde) linker with a BPDA (biphenyl 4,4'-dicarboxaldehyde), which increased the framework's porosity. In fact, the number of electroactive sites detected doubled after this change, probably due to the new framework's sites having both higher electrochemical and chemical accessibilities.

Once the porosity was tuned and the catalytic activity improved, Lin *et al.* then aimed to further improve the proportion of active sites, the quantity of which is thought to be limited by the poor electrochemical contact between the COF and the electrode. Thus, the morphology of the COF was modified by growing highly oriented thin films on the electrode. The COF thin-film was characterised by a higher conductivity, higher currents and a higher diffusion coefficient of the system overall compared to the previous study. Also, the electrocatalytic efficiency was improved under the same conditions: a seven-fold increase in TOF and a higher current density with 86% FE for CO were observed. Additionally, the catalytic mechanism of the Co-porphyrin was found to be altered by its immobilisation within the COF structure. This study therefore shows a proof of concept of an efficient hybrid system realised by the mixing of features of both molecular complexes and heterogeneous systems in order to promote and control the reduction of CO₂, particularly in aqueous media and using sustainable electrical energy sources.⁷⁰

From these studies it has been elucidated that when using molecular complexes loaded on COFs the mobility of charge carriers becomes another key point. Much effort has been spent already on optimising the organic ligands employed in order to tune the activity and selectivity when molecular complexes are incorporated. However, it is important to consider the possibility of adjusting the functionalisation of the COF's organic structural linkers in order to optimise them for CO₂ electroreduction while avoiding modification of the electronic structure close to the active sites.

Diercks *et al.*⁴⁰ proposed a series of COFs with different electron-withdrawing groups in the support, which should alter the reactivity of the central active sites. In this case, again, a Co-based porphyrin was chosen as the molecular complex. The COF was orientally grown on a highly ordered pyrolytic graphite surface so that it would have good contact with the substrate and many accessible Co active sites. Previous studies have shown that the mechanism of CO₂ reduction with Co-porphyrin passes through an initial reduction of Co(II) to Co(I),⁷¹ therefore, the authors decided to functionalise the COF's linker species with electron-withdrawing groups to facilitate reduction of the Co centres. CO₂ sorption tests were carried out to exclude the possibility of electrochemical methods causing an increased storage of CO₂.

In addition, XAS analysis proved the influence of the linker functionalisation on the electronic structure of the metal centre. CPE of the COF-Co with the various functionalisation was carried out at -0.67 V vs RHE, and a trend was found with XAS and CV experiments. The electron-withdrawing moieties improve the catalytic behaviour of the systems, and the current density from CO formation increases from 45 mA.mg⁻¹ for a COF-366-Co with no functionalisation on the BDA (2,5-dimethoxyterephthaldehyde) to 65 mA.mg⁻¹ for the COF-366-F-Co where one hydrogen atom is substituted with a fluorine atom. However, when substituting all hydrogens with fluorine, an inverted trend is seen, likely due to the high hydrophobicity of the perfluorinated system, which precludes electrolyte permeation.⁷¹ To conclude, this study represents another example of a molecular complex immobilised within a porous, crystalline structure that can be engineered further at the molecular level. This molecular engineering allows the authors to manipulate the electronic structure of the overall system without directly modifying the electronic of the metal centre, which often leads to decreased activity.

This last example shows the importance of engineering defects into polymeric organic networks (PONs), such as MOFs and COFs, to develop catalytic materials for the CO₂RR. Phthalic anhydride was used as a co-monomer for the defective polymeric cobalt phthalocyanine (D-P-CoPC), which generates defects on the backbone structure. UV-Vis studies and EXAFS show the different behaviour between the defect-containing and the defect-free COF in terms of promoting the surface binding of CO₂ molecules and controlling the electronic character of the Co within the framework. Higher current densities were noted in the LSVs at -0.8 V vs RHE for the defect-containing COF. The FE for CO at -0.61 V vs RHE was increased by twice, up to 97% when comparing the defect-containing polymer and the normal one. The presence of defects could then be tuned by changing the amount of phthalic anhydride to demonstrate their influence on the CO₂RR. Indeed, a higher number of defects leads to higher CO current density and an extended stable lifetime, attributed to the turning of the electronic character of the Co phthalocyanine framework and the firmer surface binding of CO₂.⁶⁴

As a final note on COFs, another recent article from 2021 by Zhang *et al.*⁷² focussing on photocatalytic CO₂ reduction uncovers the possibility of post-synthetic metalation into COF systems to construct the molecular catalyst active sites, similar to previously discussed for MOFs. This is achieved by clever design of the COF, selection of the metal and of its complementary bis-chelate ligand. Although the systems investigated by Zhang *et al.* were not designed for or investigated under electrocatalytic conditions, such advances in methodology for the incorporation of molecular catalysts within COFs represent exciting progress in the field, hopefully enabling similar advantages as seen by Hod *et al.*⁶² for their MOF-based system.

Titania. Together with carbon-based materials, titanium dioxide has been widely used in the last two decades as a support for electrochemical applications and the CO₂RR. Its similarities with carbon materials are i) stability for electrocatalysis and ii) electronic conductivity. Unlike carbon, titanium dioxide has more substantial synergistic effects when employed for the CO₂RR with metals. Titanium dioxide (TiO₂) is mainly used in the form of powder, nanoparticles, or different nanostructures, such as nanotubes (Figure 5).⁷³

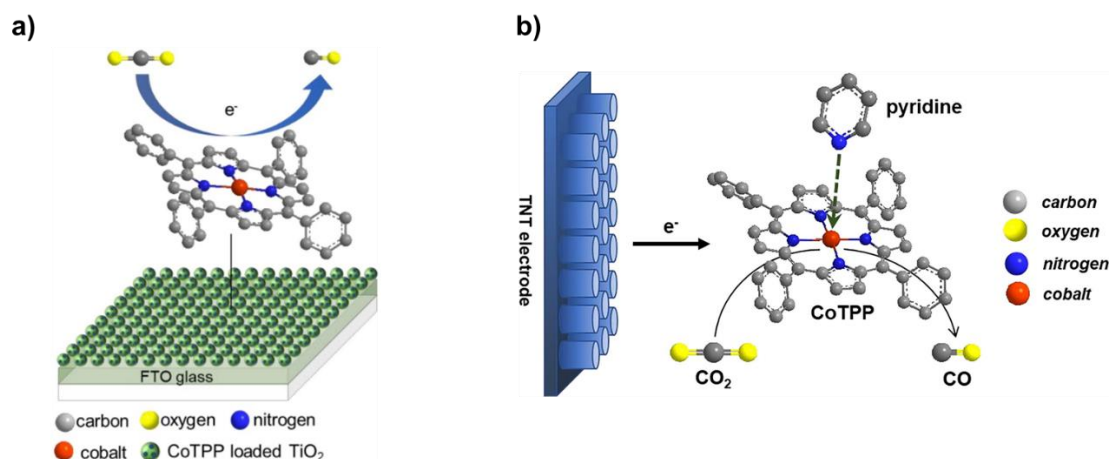


Figure 5. a) The effect of TiO₂ support for the immobilisation of molecular catalyst cobalt porphyrin on CO₂ electroreduction.⁷⁴ b) active molecular catalyst immobilised on TiO₂ nanotube electrode for CO₂ electroreduction. The axial coordination of drop-casting solvent and the porphyrin structure have significant effects on the catalytic performance.⁷⁵

DFT studies have confirmed the presence of active sites for the adsorption and activation of CO₂ at the interface between the titanium oxide and the metallic active sites. The structure of the oxide support opens new pathways for the reduction of CO₂. Despite the products formed (metal-dependent), the intermediates are expected to bind through the oxygen, thanks to the high affinity of titanium.⁷⁶ Moreover, the crystallinity of the Titania has also been proven to be a crucial factor.³⁹ Gu *et al.* prepared different titanium nanoparticles by a sol-gel method and calcined them at different temperatures to enhance their crystallinity. The different nanoparticles were then deposited on FTO glasses and a solution of a cobalt tetraphenyl porphyrin (CoTPP) was dropcast onto them. Indeed, the titanium oxide calcined at 200 and 400 °C shows anatase as the crystalline phase, whereas samples calcined at 800 °C presents a pure rutile structure and intermediate temperature calcination gives a mixed crystalline phase. The samples were studied under cyclic voltammetry (CV) in 0.5 M KHCO₃ electrolyte. An increase of current density at -1.35 V vs SHE is noted after purging with CO₂. A characteristic peak of the CoTPP complex proves the presence of the active site and the poor activity of the bare TiO₂. However, the CoTPP added to the TiO₂ obtained after calcination at 800 °C shows the lowest current density. The authors suggest these observations indicate that, when keeping the CoTPP loading constant, the variation in the electrocatalytic performances is related to the support and its calcination treatment. The highest temperature for calcination treatment seems to affect the efficiency of the system negatively. The lower efficiency of the system which was calcined at a higher temperature was caused by the lower surface coverage of active sites. The CoTPP dropcast on the titania calcined at 200 °C reaches a coverage five times larger than that dropcast on the titania treated at 800 °C. The faradaic efficiency for CO, turnover number and current density follow the same trend from 200 to 800 °C. Likewise, the support is shown to be more active in its anatase crystalline phase for

photocatalytic activity. However, although 200TiO₂ and 400TiO₂ possess the same crystalline phase, the sample calcined at 200 °C displays better activity, likely attributable to the presence of carbonaceous species. For this reason, the effect of carbon was investigated by synthesising both carbon-doped and carbon-free titania. The study reports the increase in conductivity and, therefore, current density for the system where carbon was present. Although titania was shown not to be a factor in influencing the CO₂ reduction mechanism, it does affect the conductivity of the system if the anatase phase and carbonaceous species are present. It also increases the effect of diffusion, as shown in the Tafel plot slopes. Hence, the fastest electron transfer and the best performances are achieved with carbon-doped titania systems.⁷⁴

In addition to the crystalline phase, analogous to the carbon-based materials, the titania's morphology and structure are fundamentally important in determining its properties. Indeed, Gu *et al.*⁷⁵ compared titania nanotubes (TNT) and Ti foil as supports for the immobilisation of a cobalt porphyrin (CoTPP). The amount of electroactive species present on the TNT is almost double the one present in a carbon cloth drop-casted with CoTPP with the same initial amount. In the Ti foil support, the CoTPP peak was not seen. Thus, the high specific surface area of the titania nanotubes proved to have good properties for hosting the molecular complex.

Furthermore, the catalytic properties were also studied. The CoTPP@TNT produced a high amount of CO with around 40% FE for CO at -1.10 V *vs* SHE, corresponding to a relatively low overpotential. Moreover, the TNTs improve the cost and mechanical properties of the electrode, when compared to carbon nanotubes, by virtue of being a simple solid metal sheet. Within this context, already in 2016, Rosser *et al.*⁷⁷, immobilised a Mn-based molecular complex on a mesoporous titania support by drop-casting. The system was tested for electrocatalytic solar-driven CO₂ reduction and showed an increased current density in CO₂-saturated media. This represented a FE of around 70% for CO at -1.7 V *vs* Fc/Fc⁺ with the lowest overpotential for a molecular complex in non-aqueous solvent reported at that time.

Interestingly, the HER was suppressed by loading more Mn complex, suggesting that the HER results from TiO₂ itself. It has been shown that molecular Mn complex dimers are likely to enhance the activity for CO₂RR. UV-vis and ATR-FTIR show the presence of catalytically active Mn-Mn dimers, which react with the CO₂. The immobilisation of the Mn complex on the mesoporous TiO₂ leads to a high local concentration of Mn on the surface under cathodic potential. The mesoporous titania thus gives a suitable environment for the complex to dimerise when a reductive potential is applied. The same group recently followed up on this research topic⁷⁸ by immobilising a Cobalt phthalocyanine (CoPc), again on mesoporous metal oxides electrodes. The same phosphonic functionalisation strategy was used to anchor the functionalised molecular complex (CoPcP) on the metal oxide. More specifically, mesoporous indium tin oxide (meso-ITO) and mesoporous titanium oxide (meso-TiO₂) were used to heterogenize the CoPcP by soaking the electrode in a solution of the complex. CPE was carried out using mesoTiO₂/CoPcP, yielding a maximum FE for CO of 85% with 1.3 mA.cm⁻² at -1.08 V *vs* SHE in 0.5 M KHCO₃.

These studies highlight the feasibility of cost-effective TiO₂ as possible support to immobilise active sites and achieve efficient CO₂ electroreduction in aqueous solutions.

Polymer-gel. Polymer-based supports have been recently employed for the CO₂RR to enhance the electrodes' scalability, processability, and mechanical properties. In addition to this, the possibility of incorporating functional groups onto the polymeric chain paves the way for multiple novel studies. Recently, ionic liquids (ILs) have been described as promising materials for the adsorption of CO₂. In these media, the solubility of CO₂ is markedly increased. Moreover, ILs have been highlighted for their ability to activate CO₂.^{13,79} In 2016, McNicholas *et al.*⁴¹ developed a cross-linked polymer network able to capture and reduce CO₂. The ion gel was made out of a PS-PEO-PS triblock brush polymer where 1-butyl-3-methylimidazolium bis(trifluoromethylsulfonyl)imide and [Re(bpy)(CO)₃Cl] (bpy = 2,2'-bipyridine) were encapsulated. A catalytic wave reveals the presence of CO₂ in the cyclic voltammetry analysis with a 450 mV shift of potential towards more positive potential. Although the current density in the ion-gel is shown to be lower than the one in ILs due to the slower diffusion, the material shows a lower overpotential requirement for the CO₂RR. This is probably due to the enhancement of the solubility of CO₂ in PIs. A few years later the same research group²⁶ prepared a polymer ion-gel from acrylamide using a radical polymerisation method alongside silicone rubber. Imidazolium moieties were added here, too, to improve CO₂ solubility and activation. The same catalyst was used, but this time the system was cast on a carbon cloth substrate to enhance the current density and so that the reaction could be carried out in aqueous media (Figure 6). The FE reached up to 90% for CO in a 0.1 KOH + 0.1 K₂CO₃ electrolyte, at the same potential as in organic solvent (i.e. -0.68 V vs RHE), with the current density of between 1 and 2 mA cm⁻². It is worth noting that, under the same conditions, the system without the polymer ion gel yielded mainly H₂. The system was shown to have a stable FE over 6 hours, but this decreased to 50% after 24 hours. The polymer ion gel was tested using other molecular complexes with good outcomes, demonstrating the system's versatility for CO₂ electroreduction. Indeed, the electrode was also coupled in a full cell system.²⁶ This last class of materials in particular opens up new paths towards more suitable materials for industrial applications, approaching the desired scalability, processability and mechanical properties, which are typically characteristic of polymers, but also alongside the capacity to act as a catalyst support for CO₂ electroreduction.



Figure 6. *fac*-[Re(bpy)(CO)₃Cl] ([Re–Cl]) dispersed in polymer ion gel (PIG) ([Re]–PIG) to carry out electrocatalytic CO₂ reduction in water.²⁶

Summary and outlook

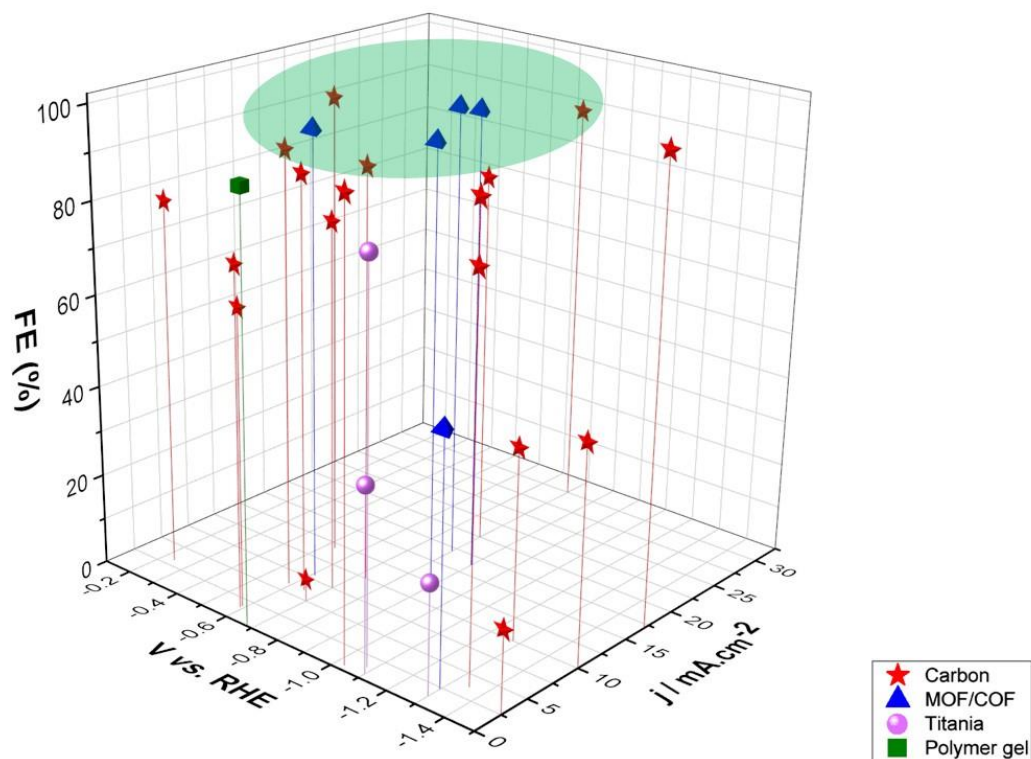


Figure 7. Graph summarising FE % vs potential applied and current density for CO₂RR products.

To summarise, we have described five different types of supports as the major ones present in the literature. Among these, the carbon-based supports (in their multiple forms), the titania supports and the MOF/COF supports are the predominant systems in literature, representing 90% of described supports for the immobilisation of molecular complexes. Therefore, we shall focus the discussion about those supports which are likely to be the most promising. Figure 7 shows an overview of selectivity efficiency for the main product compared against the current density obtained and the potential applied. Analysing the graphs carefully, we can observe the following trends:

- (i) The systems reaching the highest FE are located in the range of potential applied between -0.5 and -1.4 V vs RHE, which is relatively less negative compared to all the ranges investigated. For the titania systems, a higher applied potential is needed for the CO₂RR, namely one more negative than -1.1 V vs RHE due to the conductive band potential. However, even with higher potential, only one case reaches FE comparable with the best carbon-based electrodes. This result highlights the superiority at present of carbon-based materials over titania-based ones.

The MOF/COF-based electrodes show FE higher than 90% at relatively low potentials between -0.6 and -0.8 V *vs* RHE in most of the cases analysed. This outcome therefore also highlights the advantage of such systems in having high dispersion of the active sites thoroughly the support framework.

- (ii) In terms of current density in all the systems considered where an H-cell setup is employed, current densities between 2 and 30 mA cm⁻² are achieved for most carbon-based materials, reaching FEs higher than 65%. Titania-based materials have a current density limited to a maximum value of 1.3 mA.cm⁻², likely due to the lower electrical conductivity. Concerning MOFs/COFs, 2 out of 3 samples analysed reach current densities of above 7 mA.cm⁻², with FE approaching unity.
- (iii) Regarding the carbon materials-based supports, the most promising material in terms of a minimised overpotential requirement and a maximised FE is a system where a Co-based molecular complex is immobilised on MWCNTs.¹⁸ The electrode reaches 100% FE for CO at a potential applied of -0.53 V *vs* RHE. In terms of current density in the H-shape cell, there is also an excellent material that reaches 30 mA.cm⁻² at -0.8 V *vs* RHE by immobilising a Co phthalocyanine on defect-rich graphene oxide.⁵⁶

The points listed above and the performances of all the systems lead us to feature and commend the carbon-based materials for employment as efficient materials and supports for the immobilisation of active catalytic sites to perform the CO₂RR. Reaching high selectivity at low overpotentials and relatively high current density when a scalable electrochemical device is employed are the chief advantages. Further implementation of these systems in flow cells and more advanced systems will undoubtedly lead to improvements in the current densities. In addition to that, the novelty of using molecular complexes within the framework structures of MOFs and COFs is a promising way for future studies. In all the examples above-listed we highlight the support's influence in different key aspects of the CO₂RR, such as high and easy loadings of molecular complexes, activities and selectivities.

More studies are needed to improve those systems, mainly focusing on their electrical conductivity and morphology, boosting overall efficiency. Thus, the choice of the support, and the intelligent engineering thereof, pose critical questions that have to be addressed carefully in order to develop impressive and scalable heterogenous catalysts for the reduction of CO₂.

For this reason, additional revolutionary, in-depth experimental and computational studies to rationally design and understand the best supports for the heterogenisation of active sites are clearly called for, in order to develop new systems for CO₂RR catalysis with augmented performances and thereby attain the higher efficiencies necessary for industrial and ecological relevancy.

References

1. Friedlingstein, P. *et al.* Global Carbon Budget 2020. *Earth Syst. Sci. Data* **12**, 3269–3340 (2020).
2. Huang, C. H. & Tan, C. S. A review: CO₂ utilization. *Aerosol Air Qual. Res.* **14**, 480–499 (2014).
3. Fujita, E. Photochemical carbon dioxide reduction with metal complexes. *Coord. Chem. Rev.* **185–186**, 373–384 (1999).
4. Dai, W. L., Luo, S. L., Yin, S. F. & Au, C. T. The direct transformation of carbon dioxide to organic carbonates over heterogeneous catalysts. *Appl. Catal. A Gen.* **366**, 2–12 (2009).
5. Waki, M. *et al.* Re(bpy)(CO)₃Cl Immobilized on Bipyridine-Periodic Mesoporous Organosilica for Photocatalytic CO₂ Reduction. *Chem. - A Eur. J.* **24**, 3846–3853 (2018).
6. Al-Rowaili, F. N., Jamal, A., Ba Shammakh, M. S. & Rana, A. A Review on Recent Advances for Electrochemical Reduction of Carbon Dioxide to Methanol Using Metal-Organic Framework (MOF) and Non-MOF Catalysts: Challenges and Future Prospects. *ACS Sustain. Chem. Eng.* **6**, 15895–15914 (2018).
7. Benson, E. E., Kubiak, C. P., Sathrum, A. J. & Smieja, J. M. Electrocatalytic and homogeneous approaches to conversion of CO₂ to liquid fuels. *Chem. Soc. Rev.* **38**, 89–99 (2009).
8. Elgrishi, N., Chambers, M. B., Wang, X. & Fontecave, M. Molecular polypyridine-based metal complexes as catalysts for the reduction of CO₂. *Chem. Soc. Rev.* **46**, 761–796 (2017).
9. Fisher, B. & Eisenberg, R. Electrocatalytic Reduction of Carbon Dioxide by Using Macrocycles of Nickel and Cobalt. *J. Am. Chem. Soc.* **102**, 7361–7363 (1980).
10. Hammouche, M., Lexa, D., Savéant, J. M. & Mometeau, M. Catalysis of the electrochemical reduction of carbon dioxide by iron(0) porphyrins. *J. Electroanal. Chem.* **249**, 347–351 (1988).
11. Windle, C. D. *et al.* Improving the photocatalytic reduction of CO₂ to CO through immobilisation of a molecular Re catalyst on TiO₂. *Chem. - A Eur. J.* **21**, 3746–3754 (2015).
12. Ching, H. Y. V. *et al.* Rhenium Complexes Based on 2-Pyridyl-1,2,3-triazole Ligands: A New Class of CO₂ Reduction Catalysts. *Inorg. Chem.* **56**, 2966–2976 (2017).
13. Grammatico, D. *et al.* Immobilization of a Molecular Re Complex on MOF-derived Hierarchical Porous Carbon for CO₂ Electroreduction in Water/Ionic Liquid Electrolyte. *ChemSusChem* **13**, 6418–6425 (2020).
14. De Luna, P. *et al.* What would it take for renewably powered electrosynthesis to displace petrochemical processes? *Science* (80-.). **364**, (2019).
15. Zhang, X. *et al.* Highly selective and active CO₂ reduction electrocatalysts based on cobalt phthalocyanine/carbon nanotube hybrid structures. *Nat. Commun.* **8**, (2017).
16. Hu, X. M., Rønne, M. H., Pedersen, S. U., Skrydstrup, T. & Daasbjerg, K. Enhanced Catalytic Activity of Cobalt Porphyrin in CO₂ Electroreduction upon Immobilization on Carbon Materials. *Angew. Chemie - Int. Ed.* **56**, 6468–6472 (2017).
17. Blakemore, J. D., Gupta, A., Warren, J. J., Brunschwig, B. S. & Gray, H. B. Noncovalent immobilization of electrocatalysts on carbon electrodes for fuel production. *J. Am. Chem. Soc.* **135**, 18288–18291 (2013).

18. Wang, M., Chen, L., Lau, T. & Robert, M. Hybrid Catalysis A Hybrid Co Quaterpyridine Complex / Carbon Nanotube Catalytic Material for CO₂ Reduction in Water. *Angew. Chemie - Int. Ed.* **2**, 7769–7773 (2018).
19. Kozuch, S. & Martin, J. M. L. “Turning Over” Definitions in Catalytic Cycles. *ACS Catal.* **2**, 2787–2794 (2012).
20. Rotundo, L. *et al.* ChemComm Electrochemical CO₂ reduction in water at carbon cloth electrodes functionalized with a. 775–777 (2019). doi:10.1039/c8cc08385a
21. Wang, Y., Marquard, S. L., Wang, D., Dares, C. & Meyer, T. J. Single-Site, Heterogeneous Electrocatalytic Reduction of CO₂ in Water as the Solvent. (2017). doi:10.1021/acsenergylett.7b00226
22. Clark, M. L. *et al.* CO₂ Reduction Catalysts on Gold Electrode Surfaces Influenced by Large Electric Fields CO₂ Reduction Catalysts on Gold Electrode Surfaces Influenced by Large Electric Fields of Chemistry and Energy Sciences Institute , Yale University , 225 Prospect St . (2018). doi:10.1021/jacs.8b09852
23. Sun, C. *et al.* Electrochemical CO₂ Reduction at Glassy Carbon Electrodes Functionalized by MnI and ReI Organometallic Complexes. *ChemPhysChem* **18**, 3219–3229 (2017).
24. Nam, D. H. *et al.* Molecular enhancement of heterogeneous CO₂ reduction. *Nat. Mater.* **19**, 266–276 (2020).
25. Chambers, M. B. *et al.* Photocatalytic Carbon Dioxide Reduction with Rhodium-based Catalysts in Solution and Heterogenized within Metal–Organic Frameworks. *ChemSusChem* **8**, 603–608 (2015).
26. Sato, S., McNicholas, B. J. & Grubbs, R. H. Aqueous electrocatalytic CO₂ reduction using metal complexes dispersed in polymer ion gels. *Chem. Commun.* **56**, 4440–4443 (2020).
27. Zhu, G. *et al.* Curvature Dependent Selectivity of CO Electrocatalytic Reduction on Cobalt Porphyrin. *ACS Catal.* **6**, 6294–6301 (2016).
28. Zhang, X. *et al.* Highly selective and active CO₂ reduction electrocatalysts based on cobalt phthalocyanine/carbon nanotube hybrid structures. *Nat. Commun.* **8**, 1–8 (2017).
29. Reuillard, B. *et al.* Tuning Product Selectivity for Aqueous CO₂ Reduction with a Mn(bipyridine)-pyrene Catalyst Immobilized on a Carbon Nanotube Electrode. *J. Am. Chem. Soc.* **139**, 14425–14435 (2017).
30. Kang, P., Zhang, S., Meyer, T. J. & Brookhart, M. Rapid selective electrocatalytic reduction of carbon dioxide to formate by an iridium pincer catalyst immobilized on carbon nanotube electrodes. *Angew. Chemie - Int. Ed.* **53**, 8709–8713 (2014).
31. Marianov, A. N. & Jiang, Y. Covalent ligation of Co molecular catalyst to carbon cloth for efficient electroreduction of CO₂ in water. *Appl. Catal. B Environ.* **244**, 881–888 (2019).
32. Orchanian, N. M., Hong, L. E. & Marinescu, S. C. Immobilized Molecular Wires on Carbon-Cloth Electrodes Facilitate CO₂ Electrolysis. *ACS Catal.* **9**, 9393–9397 (2019).
33. Manuscript, A. Energy & Environmental Science. (2019). doi:10.1039/C8EE03403F
34. Choi, J. *et al.* A Porphyrin / Graphene Framework : A Highly Efficient and Robust Electrocatalyst for Carbon Dioxide Reduction. *Adv. Energy Mater.* **8**, 1801280 (2018).
35. Huang, P. *et al.* Nano Energy Single Mo atom realized enhanced CO₂ electro-reduction into formate

- on N- doped graphene. *Nano Energy* **61**, 428–434 (2019).
36. Karapinar, D. *et al.* FeNC catalysts for CO₂ electroreduction to CO: Effect of nanostructured carbon supports. *Sustain. Energy Fuels* **3**, 1833–1840 (2019).
 37. Mota, F. M. *et al.* Toward an Effective Control of the H₂ to CO Ratio of Syngas through CO₂ Electroreduction over Immobilized Gold Nanoparticles on Layered Titanate Nanosheets Toward an Effective Control of the H₂ to CO Ratio of Syngas through CO₂ Electroreduction over Imm. (2018). doi:10.1021/acscatal.8b00647
 38. Rosser, T. E., Windle, C. D. & Reisner, E. Electrocatalytic and Solar-Driven CO₂ Reduction to CO with a Molecular Manganese Catalyst Immobilized on Mesoporous TiO₂. *Angew. Chemie - Int. Ed.* **55**, 7388–7392 (2016).
 39. Li, T., Shan, B., Xu, W. & Meyer, T. J. Electrocatalytic CO₂ Reduction with a Ruthenium Catalyst in Solution and on Nanocrystalline TiO₂. *ChemSusChem* **12**, 2402–2408 (2019).
 40. Diercks, C. S. *et al.* Reticular Electronic Tuning of Porphyrin Active Sites in Covalent Organic Frameworks for Electrocatalytic Carbon Dioxide Reduction. *J. Am. Chem. Soc.* **140**, 1116–1122 (2018).
 41. McNicholas, B. J. *et al.* Electrocatalysis of CO₂ Reduction in Brush Polymer Ion Gels. *J. Am. Chem. Soc.* **138**, 11160–11163 (2016).
 42. Wakerley, D. *et al.* Bio-inspired hydrophobicity promotes CO₂ reduction on a Cu surface. *Nat. Mater.* **18**, 1–7 (2019).
 43. Varela, A. S. *et al.* Electrochemical Reduction of CO₂ on Metal-Nitrogen-Doped Carbon Catalysts. *ACS Catal.* **9**, 7270–7284 (2019).
 44. Pugliese, S. *et al.* Functionalization of Carbon Nanotubes with Nickel Cyclam for the Electrochemical Reduction of CO₂. *ChemSusChem* **13**, 6449–6456 (2020).
 45. Zhang, Q. *et al.* Electrochemical Reduction of CO₂ by SnO_x Nanosheets Anchored on Multiwalled Carbon Nanotubes with Tunable Functional Groups. *ChemSusChem* **12**, 1443–1450 (2019).
 46. Zhu, M. *et al.* Applied Catalysis B : Environmental Cobalt phthalocyanine coordinated to pyridine-functionalized carbon nanotubes with enhanced CO₂ electroreduction. *Appl. Catal. B Environ.* **251**, 112–118 (2019).
 47. Chen, X., Hu, X. M., Daasbjerg, K. & Ahlquist, M. S. G. Understanding the Enhanced Catalytic CO₂ Reduction upon Adhering Cobalt Porphyrin to Carbon Nanotubes and the Inverse Loading Effect. *Organometallics* **39**, 1634–1641 (2020).
 48. Guo, C. *et al.* How does mass transfer influence electrochemical carbon dioxide reduction reaction? A case study of Ni molecular catalyst supported on carbon. *Chem. Commun.* **1**, 1–4 (2021).
 49. Balamurugan, M. *et al.* Electrocatalytic Reduction of CO₂ to Ethylene by Molecular Cu-Complex Immobilized on Graphitized Mesoporous Carbon. *Small* **16**, 2000955 (2020).
 50. Zhu, M. *et al.* Covalently Grafting Cobalt Porphyrin onto Carbon Nanotubes for Efficient CO₂ Electroreduction. *Angew. Chemie Int. Ed.* **58**, 6595–6599 (2019).
 51. Liang, Y., Li, Y., Wang, H. & Dai, H. Strongly Coupled Inorganic/Nanocarbon Hybrid Materials for Advanced Electrocatalysis. *J. Am. Chem. Soc.* **135**, 2013–2036 (2013).
 52. Karapinar, D. *et al.* Carbon-Nanotube-Supported Copper Polyphthalocyanine for Efficient and

- Selective Electrocatalytic CO₂ Reduction to CO. *ChemSusChem* **13**, 173–179 (2020).
53. Maurin, A. & Robert, M. Noncovalent Immobilization of a Molecular Iron-Based Electrocatalyst on Carbon Electrodes for Selective, Efficient CO₂ to CO Conversion in Water. 3–6 (2016). doi:10.1021/jacs.5b12652
 54. Birdja, Y. Y. *et al.* Effects of Substrate and Polymer Encapsulation on CO₂ Electroreduction by Immobilized Indium(III) Protoporphyrin. *ACS Catal.* **8**, 4420–4428 (2018).
 55. Wang, J. *et al.* Linkage Effect in the Heterogenization of Cobalt Complexes by Doped Graphene for Electrocatalytic CO₂ Reduction. *Angew. Chemie Int. Ed.* **58**, 13532–13539 (2019).
 56. Liang, F. *et al.* Intrinsic Defect-Rich Graphene Coupled Cobalt Phthalocyanine for Robust Electrochemical Reduction of Carbon Dioxide. *ACS Appl. Mater. Interfaces* **13**, 25523–25532 (2021).
 57. König, M., Vaes, J., Klemm, E. & Pant, D. Solvents and Supporting Electrolytes in the Electrocatalytic Reduction of CO₂. *iScience* **19**, 135–160 (2019).
 58. Zheng, X. *et al.* Bio-inspired Murray materials for mass transfer and activity. *Nat. Commun.* **8**, 14921 (2017).
 59. Yang, K. D. *et al.* Morphology-Directed Selective Production of Ethylene or Ethane from CO₂ on a Cu Mesopore Electrode. *Angew. Chem. Int. Ed. Engl.* **56**, 796–800 (2017).
 60. Zhanaidarova, A., Jones, S. C., Despagnet-Ayoub, E., Pimentel, B. R. & Kubiak, C. P. Re(tBu-bpy)(CO)₃Cl Supported on Multi-Walled Carbon Nanotubes Selectively Reduces CO₂ in Water. *J. Am. Chem. Soc.* **141**, 17270–17277 (2019).
 61. Heidary, N., Harris, T. G. A. A., Ly, K. H. & Kornienko, N. Artificial photosynthesis with metal and covalent organic frameworks (MOFs and COFs): challenges and prospects in fuel-forming electrocatalysis. *Physiol. Plant.* **166**, 460–471 (2019).
 62. Hod, I. *et al.* Fe-Porphyrin-Based Metal-Organic Framework Films as High-Surface Concentration, Heterogeneous Catalysts for Electrochemical Reduction of CO₂. *ACS Catal.* **5**, 6302–6309 (2015).
 63. Hui, S. R. & Luna, P. De. How increasing proton and electron conduction benefits electrocatalytic CO₂ reduction. *Matter* **4**, 1555–1577 (2021).
 64. Wu, H. *et al.* Defect Engineering in Polymeric Cobalt Phthalocyanine Networks for Enhanced Electrochemical CO₂ Reduction. *ChemElectroChem* **5**, 2717–2721 (2018).
 65. Wang, Y. R. *et al.* Oriented electron transmission in polyoxometalate-metalloporphyrin organic framework for highly selective electroreduction of CO₂. *Nat. Commun.* **9**, 1–8 (2018).
 66. Wang, C., Xie, Z., deKrafft, K. E. & Lin, W. Doping Metal–Organic Frameworks for Water Oxidation, Carbon Dioxide Reduction, and Organic Photocatalysis. *J. Am. Chem. Soc.* **133**, 13445–13454 (2011).
 67. Senthil Kumar, R., Senthil Kumar, S. & Anbu Kulandainathan, M. Highly selective electrochemical reduction of carbon dioxide using Cu based metal organic framework as an electrocatalyst. *Electrochem. commun.* **25**, 70–73 (2012).
 68. Kornienko, N. *et al.* Metal–Organic Frameworks for Electrocatalytic Reduction of Carbon Dioxide. *J. Am. Chem. Soc.* **137**, 14129–14135 (2015).
 69. Yao, C. L., Li, J. C., Gao, W. & Jiang, Q. An Integrated Design with new Metal-Functionalized

- Covalent Organic Frameworks for the Effective Electroreduction of CO₂. *Chem. - A Eur. J.* **24**, 11051–11058 (2018).
70. Lin, S. *et al.* Covalent organic frameworks comprising cobalt porphyrins for catalytic CO₂ reduction in water. *Science* (80-.). 2015, 349, 1208–1213. *Science* (80-.). **349**, 1208–1213 (2015).
 71. Leung, K., Nielsen, I. M. B., Sai, N., Medforth, C. & Shelnutt, J. A. Cobalt-porphyrin catalyzed electrochemical reduction of carbon dioxide in water. 2. Mechanism from first principles. *J. Phys. Chem. A* **114**, 10174–10184 (2010).
 72. Yang, Y. *et al.* Decoration of Active Sites in Covalent–Organic Framework: An Effective Strategy of Building Efficient Photocatalysis for CO₂ Reduction. *ACS Sustain. Chem. Eng.* **9**, 13376–13384 (2021).
 73. Lavacchi, A. *et al.* Titanium dioxide nanomaterials in electrocatalysis for energy. *Curr. Opin. Electrochem.* **28**, 100720 (2021).
 74. Gu, S., Marianov, A. N., Xu, H. & Jiang, Y. Effect of TiO₂ support on immobilization of cobalt porphyrin for electrochemical CO₂ reduction. *J. Mater. Sci. Technol.* **80**, 20–27 (2021).
 75. Gu, S., Marianov, A. N., Zhu, Y. & Jiang, Y. Cobalt porphyrin immobilized on the TiO₂ nanotube electrode for CO₂ electroreduction in aqueous solution. *J. Energy Chem.* **55**, 219–227 (2021).
 76. Zhai, L. *et al.* Titania-Modified Silver Electrocatalyst for Selective CO₂ Reduction to CH₃OH and CH₄ from DFT Study. *J. Phys. Chem. C* **121**, 16275–16282 (2017).
 77. Rosser, T. E., Windle, C. D. & Reisner, E. Electrocatalytic and Solar-Driven CO₂ Reduction to CO with a Molecular Manganese Catalyst Immobilized on Mesoporous TiO₂. *Angew. Chemie - Int. Ed.* **55**, 7388–7392 (2016).
 78. Roy, S. *et al.* Electrocatalytic and Solar-Driven Reduction of Aqueous CO₂ with Molecular Cobalt Phthalocyanine–Metal Oxide Hybrid Materials. *ACS Catal.* **11**, 1868–1876 (2021).
 79. Rosen, B. A. *et al.* Ionic liquid-mediated selective conversion of CO₂ to CO at low overpotentials. *Science* **334**, 643–644 (2011).